Engineering Analysis with Boundary Elements 33 (2009) 120–127

Contents lists available at ScienceDirect

Engineering Analysis with Boundary Elements

journal homepage: www.elsevier.com/locate/enganabound

A meshless hybrid boundary-node method for Helmholtz problems

Y. Miao *, Y. Wang, Y.H. Wang

School of Civil Engineering and Mechanics, Huazhong University of Science and Technology, Wuhan 430074, Hubei, PR China

ARTICLE INFO

Article history:
Received 7 January 2008
Accepted 22 May 2008
Available online 12 August 2008

Keywords:
Meshless method
Dual reciprocity-hybrid boundary node method
Helmholtz equation
Moving least squares approximation

ABSTRACT

By coupling the moving least squares (MLS) approximation with a modified functional, the hybrid boundary node-method (hybrid BNM) is a boundary-only, truly meshless method. Like boundary element method (BEM), an initial restriction of the present method is that non-homogeneous terms accounting for effects such as distributed loads are included in the formulation by means of domain integrals, and thus make the technique lose the attraction of its 'boundary-only' character.

This paper presents a new boundary-type meshless method dual reciprocity-hybrid boundary node method (DR-HBNM), which is combined the hybrid BNM with the dual reciprocity method (DRM) for solving Helmholtz problems. In this method, the solution of Helmholtz problem is divided into two parts, i.e. the complementary solution and the particular solution. The complementary solution is solved by means of hybrid BNM and the particular one is obtained by DRM. The modified variational formulation is applied to form the discrete equations of hybrid BNM. The MLS is employed to approximate the boundary variables, while the domain variables are interpolated by fundamental solutions. The domain integration is interpolated by radial basis function (RBF). The proposed method in the paper retains the characteristics of the meshless method and BEM, which only requires discrete nodes constructed on the boundary of a domain, several nodes in the domain are needed just for the RBF interpolation. The parameters that influence the performance of this method are studied through numerical examples and known analytical fields. Numerical results for the solution of Helmholtz equation show that high convergence rates and high accuracy are achievable.

1. Introduction

The Helmholtz equation, $\nabla^2 u + \mu^2 u = 0$, is an elliptic partial differential equation which is a time-harmonic solution of the wave equation. The Helmholtz equation governs some important physical phenomena. These include the vibration of a structure [1], the acoustic cavity problem [2], the radiation wave [3] and the scattering of a wave [4]. Obtaining an efficient and more accurate numerical solution for the Helmholtz equation has been the subject of many studies.

In the last decades, the dual reciprocity-BEM (DR-BEM) [5] and multiple reciprocity-BEM (MR-BEM) [6] have been emerging as two most promising BEM techniques to handle inhomogeneous problems, such as Helmholtz problems. It is well known that unlike the DR-BEM, the MR-BEM does not require internal nodes for general inhomogeneous problems. However, the drawback of the MR-BEM is that it requires more computational efforts and not easily applied to non-linear problems [7]. Another drawback is that it has much difficulty in solving problems involving changing domains such as deformation and crack propagation.

In this study, we introduce the dual reciprocity-hybrid boundary node method (DR-HBNM), a new exact boundary-only discretization technique based on hybrid boundary node-method (hybrid BNM) and dual reciprocity principle. Boundary node method is first proposed by Mukherjee [8], which is applied MLS to the boundary integration equations. Although this method does not require an element mesh for the interpolation of the boundary variables, a background element is still necessary for integration. Based on it, the hybrid BNM is proposed by Zhang [9–12], which has combined the modified functional and MLS [13] approximation. It gets rid of the background elements and achieves a truly meshless method. It uses MLS to approximate the boundary variables, and the integration is limited to a fixed local region. Elements are not required for either interpolation or integration. This method, however, can only be used for solving homogeneous problems. For the inhomogeneous problem or dynamic problem, the domain integration is inevitable.

The governing equation of Helmholtz problems has an inhomogeneous term. Hybrid BNM cannot solve them without domain integral. An initial restriction of hybrid BNM is that the fundamental solution for the original partial differential equation

* Corresponding author. Tel.: +86 27 87540172; fax: +86 27 87542231.
E-mail addresses: my_miaoyu@163.com, yhwang0062@163.com (Y. Miao).

0955-7997/$ - see front matter Crown Copyright © 2008 Published by Elsevier Ltd. All rights reserved.
doi:10.1016/j.enganabound.2008.05.009

is required to obtain a local integral equation. The inhomogeneous terms accounting distributed loads and time-dependent term are included in the formula of the domain integrals. Thus, the method loses the attraction of its 'boundary-only' and truly meshless method character.

DRM is introduced by Nardini and Brebbia [14] for elastodynamic problems in 1982 and extended by Wrobel and Brebbia [15] to time-dependent diffusion in 1986. The method is essentially a generalized way of constructing particular solution that can be used to solve the non-linear and time-dependent problems as well as to represent any internal source distribution. The method can be applied to define sources over the whole domain or only on part of it. The aim of DRM is to avoid the domain integral that comes out from the inhomogeneous term of the equations. DRM takes advantage of this fact and builds an approximated particular solution in terms of a linear combination of the RBF.

In this paper, a truly meshless method is developed for Helmholtz problem. The method is formed by the combination of hybrid BNM and DRM. The solution of Helmholtz problem composes two parts: complementary solution and particular solution. For the first part, the same as hybrid BNM, the variables inside the domain are interpolated by the fundamental solution while the unknown boundary variables are approximated by the MLS approximation. The modified variational formulation is applied to form the discrete equations of hybrid BNM. For the second part, DRM has been used and the RBFs are applied to interpolate the inhomogeneous part of the equations. Because of inhomogeneous term of the governing equations, the boundary integral equations obtained by DR-HBNM are not enough to solve all solution variables. Some additional equations are proposed to obtain the relation of the variables in the domain and on the boundary. They are obtained by interpolation of the fundamental solution and the basis type of the particular solutions, and no integrals or elements are required. In order to overcome the singular integration, the rigid body-moving method has been applied. The basic idea of this approach is to employ a fundamental solution corresponding to a simpler equation and to treat the remaining terms, as well as other non-homogeneous terms in the original equation. The internal nodes are just for RBF interpolation. So, a 'boundary-only' and truly meshless method for solving Helmholtz problems is achievable.

The discussions of this method are arranged as follows: a review of the hybrid BNM will be discussed in Section 2. DR-HBNM for Helmholtz problems is developed in Section 3. Numerical examples for Helmholtz problems are shown in Section 4. Finally, the paper will be ending with conclusions in Section 5.

2. Review of the hybrid BNM

This section gives a brief review of the hybrid BNM. For convenience, the Helmholtz-type equation is written as

$$\nabla^2 u = -\mu^2 u \tag{1}$$

in which μ is natural frequency and u is the displacement of each node.

As a consequence, the left-hand side of Eq. (1) can be dealt with by hybrid BNM for the Laplace equation, and the integrals corresponding to the right-hand side are taken into the boundary using RBF interpolation. In DR-HBNM, the solution variables u can be divided into complementary solutions u^c and particular solutions u^p, i.e.

$$u = u^c + u^p \tag{2}$$

The particular solution u^p just needs to satisfy the inhomogeneous equation in total space as follows:

$$\nabla^2 u^p = -\mu^2 u \tag{3}$$

The complementary solution u^c must satisfy the Laplace equation and the modified boundary condition, so those are written in the form

$$\nabla^2 u^c = 0 \tag{4}$$

$$u^c = \bar{u}^c = \bar{u} - u^p \tag{5}$$

$$t^c = \bar{t}^c = \bar{t} - t^p \tag{6}$$

in which $\bar{u}$, $\bar{t}$ are the boundary-node values of each node on the boundary, and $\bar{u}^c$, $\bar{t}^c$ are the generous solution of boundary nodes.

In the following, the complementary solution will be solved by the hybrid BNM.

The hybrid BNM is based on a modified variational principle. The functions in the modified principle assumed to be independent are: displacement field within the domain, u, boundary-displacement field, $\tilde{u}$, and boundary normal flux, $\tilde{t}$. Consider a domain Ω enclosed by $\Gamma = \Gamma_u + \Gamma_t$ with prescribed displacement $\bar{u}$ and normal flux $\bar{t}$ at the boundary portions Γ_u and Γ_t, respectively. The corresponding variational function $\prod_{AB}$ is defined as

$$\Pi_{AB} = \int_\Omega \frac{1}{2} u_{,i} u_{,i}\, \mathrm{d}\Omega - \int_\Gamma \tilde{t}(u - \tilde{u})\, \mathrm{d}\Gamma - \int_{\Gamma_t} \bar{t}\tilde{u}\, \mathrm{d}\Gamma \tag{7}$$

where $\tilde{t}$ and $\tilde{u}$ are the boundary-node values which are approximated by MLS, u is the internal node value, and the boundary displacement $\tilde{u}$ satisfies the essential boundary condition, i.e. $\bar{u} = \tilde{u}$, on Γ_u.

With the vanishing of $\delta \prod_{AB}$ over the domain and its boundary, the following equivalent integral can be obtained:

$$\int_\Gamma (t - \tilde{t})\, \delta\tilde{u}\, \mathrm{d}\Gamma - \int_\Omega u_{,ii}\, \delta\tilde{u}\, \mathrm{d}\Omega = 0 \tag{8}$$

$$\int_\Gamma (u - \tilde{u})\, \delta\tilde{t}\, \mathrm{d}\Gamma = 0 \tag{9}$$

$$\int_{\Gamma_t} (\tilde{t} - \bar{t})\, \delta\tilde{u}\, \mathrm{d}\Gamma = 0. \tag{10}$$

Eq. (10) will be satisfied if the traction boundary condition, $\tilde{t} = \bar{t}$, is imposed. So it will be ignored in the following.

Eqs. (8) and (9) hold for any portion of the domain Ω, for example, a sub-domain Ω_s, which is defined as an intersection of a domain and a small circle centered at node S_I, and its boundary, Γ_s and L_s. (see Fig. 1).

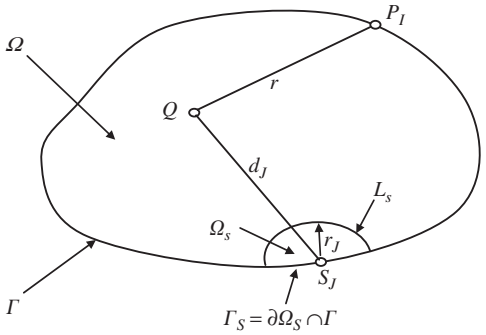

Fig. 1. Local domain and source point of fundamental solution corresponding to S_J.

So, we can use the following weak form for the sub-domain and its boundary to replace Eqs. (8) and (9):

$$\int_{\Gamma_s+L_s}(t-\tilde{t}_s)h\,\mathrm{d}\Gamma-\int_{\Omega_s}u_{,ii}h\,\mathrm{d}\Omega=0 \tag{11}$$

$$\int_{\Gamma_s+L_s}(u-\tilde{u}_s)h\,\mathrm{d}\Gamma=0 \tag{12}$$

where h is a test function. We approximate $\tilde{u}_s$ and $\tilde{t}_s$ at the boundary Γ by the MLS approximation, as

$$\tilde{u}(s)=\sum_{I=1}^{N}\Phi_I(s)\hat{u}_I \tag{13}$$

$$\tilde{t}(s)=\sum_{I=1}^{N}\Phi_I(s)\hat{t}_I \tag{14}$$

where N stands for the number of nodes located on the surface; $\hat{u}_I$ and $\hat{t}_I$ are the nodal values, and $\Phi_I(s)$ is the shape function of the MLS approximation, corresponding to node S_I, which is given by

$$\Phi_I(s)=\sum_{j=1}^{m}p_j(s)[A^{-1}(s)B(s)]_{jI} \tag{15}$$

In the above equation, $p_j(s)$ provide a basis function of order m. In this study, we take m to 3, namely, $\mathbf{p}^{\mathrm{T}}(s)=\begin{bmatrix}1, & s, & s^2\end{bmatrix}$. Matrices $A(\mathbf{s})$ and $B(\mathbf{s})$ are defined as

$$A(s)=\sum_{I=1}^{N}w_I(s)p(s_I)p^{\mathrm{T}}(s_I) \tag{16}$$

$$B(s)=[w_1(s)\,p(s_1),\ w_2(s)\,p(s_2),\ldots,w_N(s)\,p(s_N)] \tag{17}$$

In Eqs. (16) and (17), $w_I(s)$ are weight functions. Gaussian weight function corresponding to node s_I can be written as

$$w_I(s)=\begin{cases}\dfrac{\exp[-(d_I/c_I)^2]-\exp[-(\hat{d}_I/c_I)^2]}{1-\exp[-(\hat{d}_I/c_I)^2]} & 0\leqslant d_I\leqslant\hat{d}_I\\ 0 & d_I\geqslant\hat{d}_I\end{cases} \tag{18}$$

where $d_I=|s-s_I|$ is the distance between an evaluation point and node. s_I, c_I are constants controlling the shape of the weight function w_I and $\hat{d}_I$ is the size of the support domain for the weight function w_I and it determines the support of node s_I.

In Eqs. (11) and (12), $\tilde{u}_s$ and $\tilde{t}_s$ at Γ_s can be represented by $\tilde{u}$ and $\tilde{t}$ expressed in Eqs. (13) and (14) since Γ_s is a portion of Γ, while $\tilde{u}_s$ and $\tilde{t}_s$ at L_s have not been defined yet. To solve this problem, we select h such that all integrals vanish over L_s. This can be easily accomplished by using the weight function in the MLS approximation for h, with the half-length of the major axis d_I of the support of the weight function being replaced by the radius of the sub-domain Ω_s, i.e.

$$h_J(Q)=\begin{cases}\dfrac{\exp[-(d_J/c_J)^2]-\exp[-(r_J/c_J)^2]}{1-\exp[-(r_J/c_J)^2]} & 0\leqslant d_J\leqslant r_J\\ 0 & d_J\geqslant r_J\end{cases} \tag{19}$$

where d_J is the distance between point Q in the domain and the nodal point s_J. On L_s, $d_J=r_J$, from Eq. (19) it can be seen that $h_J(Q)=0$, so it vanishes on boundary L_s. Eqs. (11) and (12) can be rewritten as

$$\int_{\Gamma_s}(t-\tilde{t})h\,\mathrm{d}\Gamma-\int_{\Omega_s}u_{,ii}h\,\mathrm{d}\Omega=0 \tag{20}$$

$$\int_{\Gamma_s}(u-\tilde{u})h\,\mathrm{d}\Gamma=0 \tag{21}$$

Making use of fundamental solutions, we interpolate u inside the domain by

$$u=\sum_{I=1}^{N}u_I^s x_I \tag{22}$$

and hence at a boundary node, the normal flux is given by

$$t=\sum_{I=1}^{N}\frac{\partial u_I^s}{\partial n}x_I \tag{23}$$

where $u_I{}^s$ is the fundamental solution, x_I are unknown parameters, N is the total number of boundary nodes, n is the outward normal vector to the boundary Γ. The fundamental solution is written as

$$u_I^s=\frac{\ln r(Q,s_I)}{2\pi} \tag{24}$$

where Q and s_I are field point and source point, respectively. r is the distance between source point s_I and field point Q.

As u is expressed by Eq. (22), the last integral on the left-hand side of Eq. (20) vanishes if one does not include node s_I, at which the singularity occurs, from the sub-domain Ω_s. This singularity will be taken into account when the boundary integrals are evaluated. By substituting Eqs. (13), (14), (19), (22) and (23) into Eqs. (20) and (21), and omitting the vanishing terms, we have

$$\sum_{I=1}^{N}\int_{\Gamma_s}\frac{\partial u_I^s}{\partial n}h_J(Q)x_I\,\mathrm{d}\Gamma=\sum_{I=1}^{N}\int_{\Gamma_s}\Phi_I(s)h_J(Q)\hat{t}_I\,\mathrm{d}\Gamma \tag{25}$$

$$\sum_{I=1}^{N}\int_{\Gamma_s}u_I^s h_J(Q)x_I\,\mathrm{d}\Gamma=\sum_{I=1}^{N}\int_{\Gamma_s}\Phi_I(s)h_J(Q)\hat{u}_I\,\mathrm{d}\Gamma \tag{26}$$

Using the above equations for all nodes, one can get the system equations

$$\mathbf{TX}=\mathbf{H}\hat{\mathbf{t}}^c \tag{27}$$

$$\mathbf{UX}=\mathbf{H}\hat{\mathbf{u}}^c \tag{28}$$

where

$$U_{IJ}=\int_{\Gamma_s}u_I^s h_J(Q)\,\mathrm{d}\Gamma \tag{29}$$

$$T_{IJ}=\int_{\Gamma_s}\frac{\partial u_I^s}{\partial n}h_J(Q)\,\mathrm{d}\Gamma \tag{30}$$

$$H_{IJ}=\int_{\Gamma_s}\Phi_I(s)h_J(Q)\,\mathrm{d}\Gamma \tag{31}$$

3. The DR-HBNM

As an extension of the hybrid BNM, the main idea of the DR-HBNM consists of employing the fundamental solution corresponding to a simpler equation and considering the remaining terms of the original equation via a procedure which involves a series expansion using RBF and the reciprocity principles. In the past section, the complementary solution has been solved successfully by hybrid BNM, in this section, the DRM will be developed to solve the particular solution.

3.1. DRM

The DRM can be used in Helmholtz problem to transform the domain integral arising from the application of inhomogeneous into equivalent boundary integrals. Applying interpolation for inhomogeneous term, the following approximation can be

proposed for the term $-\mu^2 u$.

$$-\mu^2 u \approx \sum_{j=1}^{N+L} f^j \alpha^j \tag{32}$$

where the α^j are a set of initially unknown coefficients, the f^j are approximation functions. N and L are the total number of boundary nodes and total number of interior nodes, respectively.

Same as Eq. (32), the particular solution can be interpolated by the basis form of the particular solution. It can be written as follows:

$$u_I^p \approx \sum_{j=1}^{N+L} \bar{\bar{u}}_I^j \alpha^j \tag{33}$$

where $\bar{\bar{u}}_I^j$ is the basis form of particular solution.

If u^p satisfies Eq. (3), the following equations can be obtained:

$$\nabla^2 \bar{\bar{u}}^j = f^j \tag{34}$$

The approximation function, f^j, can be chosen as $f^j = 1+r+r^2$. Obviously, the particular solution $\bar{\bar{u}}$ satisfying Eq. (34) can be obtained as

$$\bar{\bar{u}} = \frac{r^2}{4} + \frac{r^3}{9} + \frac{r^4}{16} \tag{35}$$

The corresponding expression for the normal flux $\bar{\bar{t}}$ is

$$\bar{\bar{t}} = \left(r_{,x} \frac{\partial x}{\partial n} + r_{,y} \frac{\partial y}{\partial n} \right) \left(\frac{1}{2} + \frac{r}{3} + \frac{r^2}{4} \right) \tag{36}$$

Solving Eqs. (32)–(34), the particular solution can be written in matrix form as follows:

$$\mathbf{u}^p = -\mu^2 \bar{\bar{\mathbf{u}}} \mathbf{F}^{-1} \mathbf{u} \tag{37}$$

$$\mathbf{t}^p = -\mu^2 \bar{\bar{\mathbf{t}}} \mathbf{F}^{-1} \mathbf{u} \tag{38}$$

where each column of $\mathbf{F}$ consists of a vector f^j containing the values of the function f^j at the DRM collocation nodes. $\bar{\bar{\mathbf{u}}}$ and $\bar{\bar{\mathbf{t}}}$ are the matrix forms of the basis type of particular solutions.

3.2. DR-HBNM

For a well-posed problem, either $\tilde{u}$ or $\tilde{t}$ is known at each node on the boundary. However, transformation between $\hat{u}_I$ and $\tilde{u}_I$. $\hat{t}_I$ and $\tilde{t}_I$ is necessary because the MLS approximation lacks the delta function property. For the panels where $\tilde{u}_I$ is prescribed, $\tilde{u}_I$ is related to $\hat{u}_I$ by [16]

$$\hat{u}_I = \sum_{J=1}^{N_t} R_{IJ} \tilde{u}_J = \sum_{J=1}^{N_t} R_{IJ} \bar{u}_J \tag{39}$$

and for the panels where $\tilde{t}_I$ is prescribed, $\hat{t}_I$ is related to $\tilde{t}_I$ by

$$\hat{t}_I = \sum_{J=1}^{N_t} R_{IJ} \tilde{t}_J = \sum_{J=1}^{N_t} R_{IJ} \bar{t}_J \tag{40}$$

where $R_{IJ} = [\Phi_J(s_I)]^{-1}$, N_t is the total number on a piece of the edge, and $\bar{u}_J$ and $\bar{t}_j$ are the related nodal values.

Substituting Eqs. (37)–(40) into Eq. (2), then substituting the result into Eqs. (27) and (28), we can obtain

$$\mathbf{U}\mathbf{x} = \mathbf{H}\mathbf{R}(\mathbf{u} - \mathbf{u}^p) = \mathbf{H}\mathbf{R}(\mathbf{u} + \mu^2 \bar{\bar{\mathbf{u}}} \mathbf{F}^{-1} \mathbf{u}) \tag{41}$$

$$\mathbf{T}\mathbf{x} = \mathbf{H}\mathbf{R}(\mathbf{t} - \mathbf{t}^p) = \mathbf{H}\mathbf{R}(\mathbf{t} + \mu^2 \bar{\bar{\mathbf{t}}} \mathbf{F}^{-1} \mathbf{u}) \tag{42}$$

Eqs. (41) and (42) are the system equations of the DR-HBNM for Helmholtz problem. Assuming that N nodes are located on the boundary, we can get N unknown variables on the boundary from Eqs. (41) and (42). However, the equations above include the displacement of the L internal nodes, and so the additional equations are needed.

3.3. Additional equations

Eqs. (41) and (42) cannot be solved for the variables of the internal nodes and additional equations for Helmholtz problem will be developed in this section.

The unknown variables of the internal nodes can be expressed as follows:

$$u^* = u^c + u^p \tag{43}$$

The complementary solution, u^c, can be interpolated by the fundamental solution and the particular solution, u^p, can be expressed by Eq. (37). So, Eq. (43) can be rewritten as

$$\mathbf{u}^* = \mathbf{u}^s \mathbf{x} - \mu^2 \bar{\bar{\mathbf{u}}} \mathbf{F}^{-1} \mathbf{u} \tag{44}$$

where $\mathbf{u}^*$ is the displacement of the internal nodes, $\mathbf{u}^s$ is the matrix of the fundamental solution on each internal nodes and $\bar{\bar{\mathbf{u}}}$ is the matrix of values of basis type of particular solution.

Solving out the coefficient vector $\mathbf{x}$ in Eq. (41), we can obtain

$$\mathbf{x} = \mathbf{U}^{-1}\mathbf{H}\mathbf{R}(\mathbf{u} + \mu^2 \bar{\bar{\mathbf{u}}} \mathbf{F}^{-1} \mathbf{u}) \tag{45}$$

Substituting Eq. (45) into Eq. (44), we get

$$\mathbf{u}^* = \mathbf{u}^s \mathbf{U}^{-1} \mathbf{H}\mathbf{R}\mathbf{u} + \mu^2 \mathbf{u}^s \mathbf{U}^{-1} \mathbf{H}\mathbf{R} \bar{\bar{\mathbf{u}}} \mathbf{F}^{-1} \mathbf{u} - \mu^2 \bar{\bar{\mathbf{u}}} \mathbf{F}^{-1} \mathbf{u} \tag{46}$$

Substituting Eq. (45) into Eq. (42), we get

$$\mathbf{T}\mathbf{U}^{-1}\mathbf{H}\mathbf{R}(\mathbf{u} + \mu^2 \bar{\bar{\mathbf{u}}} \mathbf{F}^{-1} \mathbf{u}) = \mathbf{H}\mathbf{R}(\mathbf{t} + \mu^2 \bar{\bar{\mathbf{t}}} \mathbf{F}^{-1} \mathbf{u}) \tag{47}$$

Combining Eq. (46) with Eq. (47), one can obtain

$$\mathbf{u}\hat{\mathbf{H}} - \mathbf{t}\hat{\mathbf{G}} = -\mu^2 \mathbf{S}\mathbf{u} \tag{48}$$

where

$$\hat{\mathbf{H}} = \begin{bmatrix} \mathbf{T}\mathbf{U}^{-1}\mathbf{H}\mathbf{R} & 0 \\ \mathbf{u}^s \mathbf{U}^{-1}\mathbf{H}\mathbf{R} & -\mathbf{I} \end{bmatrix} \tag{49}$$

$$\hat{\mathbf{G}} = \begin{Bmatrix} \mathbf{H}\mathbf{R} \\ 0 \end{Bmatrix} \tag{50}$$

$$\mathbf{S} = \begin{Bmatrix} \mathbf{T}\mathbf{U}^{-1}\mathbf{H}\mathbf{R}\bar{\bar{\mathbf{u}}}\mathbf{F}^{-1} - \mathbf{H}\mathbf{R}\bar{\bar{\mathbf{t}}}\mathbf{F}^{-1} \\ \mathbf{u}^s \mathbf{U}^{-1}\mathbf{H}\mathbf{R}\bar{\bar{\mathbf{u}}}\mathbf{F}^{-1} - \bar{\bar{\mathbf{u}}}\mathbf{F}^{-1} \end{Bmatrix} \tag{51}$$

Take a standard Helmholtz problem, a vibrating beam, as an example. The external loads are set to zero, and the boundary condition of displacement is also set to zero, i.e.

$$\mathbf{u}_1 = \{0\}, \quad \mathbf{t}_2 = \{0\} \tag{52}$$

Imposed the boundary condition, Eq. (48) can be assembled into the following system of equations:

$$\begin{bmatrix} \hat{\mathbf{H}}_{11} & \hat{\mathbf{H}}_{12} \\ \hat{\mathbf{H}}_{21} & \hat{\mathbf{H}}_{22} \end{bmatrix} \begin{bmatrix} 0 \\ \mathbf{u} \end{bmatrix} - \begin{bmatrix} \hat{\mathbf{G}}_{11} & \hat{\mathbf{G}}_{12} \\ \hat{\mathbf{G}}_{21} & \hat{\mathbf{G}}_{22} \end{bmatrix} \begin{bmatrix} \mathbf{t} \\ 0 \end{bmatrix} = -\mu^2 \begin{bmatrix} \mathbf{S}_{11} & \mathbf{S}_{12} \\ \mathbf{S}_{21} & \mathbf{S}_{22} \end{bmatrix} \begin{bmatrix} 0 \\ \mathbf{u} \end{bmatrix} \tag{53}$$

or

$$\hat{\mathbf{H}}_{12}\mathbf{u} - \hat{\mathbf{G}}_{11}\mathbf{t} = -\mu^2 \mathbf{S}_{12}\mathbf{u} \tag{54}$$

$$\hat{\mathbf{H}}_{22}\mathbf{u} - \hat{\mathbf{G}}_{21}\mathbf{t} = -\mu^2 \mathbf{S}_{22}\mathbf{u} \tag{55}$$

Eliminating t in Eqs. (54) and (55) give

$$\mathbf{K}\mathbf{u} = \mu^2 \mathbf{M}\mathbf{u} \tag{56}$$

where

$$\mathbf{K} = \hat{\mathbf{H}}_{22} - \hat{\mathbf{G}}_{21}\hat{\mathbf{G}}_{11}^{-1}\hat{\mathbf{H}}_{12} \tag{57}$$

$$\mathbf{M} = -(\mathbf{S}_{22} - \hat{\mathbf{G}}_{21}\hat{\mathbf{G}}_{11}^{-1}\mathbf{S}_{12}) \tag{58}$$

K and **M** represent stiffness and mass matrix, respectively. Eq. (54) represents a generalized algebraic eigenvalue/eigenvector problem, the solution of which can be obtained directly by a variant of the subspace iteration scheme.

A method proposed by Nardini and Brebbia, in the context of elasticity problems, is to reduce the generalized eigenvalue problem to a standard one by inversion of matrix **K**, obtaining $\mathbf{Au} = \boldsymbol{\lambda}\mathbf{u}$ with $\mathbf{A} = \mathbf{K}^{-1}\mathbf{M}$ and $\boldsymbol{\lambda} = 1/\boldsymbol{\mu}^2$. Matrix **A** was then transformed into three-diagonal form by the Householder algorithm, and the eigenvalues and eigenvectors of the transformed matrix were found by the Q-R algorithm. All the above solution procedures may present difficulties since matrix **A** is non-symmetric and as a consequence, some of the eigenvalues will be complex. Nardini and Brebbia found that the complex eigenvalues, if present, appear in the higher modes, which are normally of less importance. In any case, problems with higher order vibration modes are inevitable when representing a continuum problem by a finite number of degrees of freedom.

Like other hybrid models (for example, the hybrid boundary element method), the present method has a drawback of 'boundary-layer effect' (the accuracy of the results in the vicinity of the boundary is very sensitive to the proximity of the interior points to the boundary). To avoid this drawback, an adaptive integration scheme has been proposed in [17]. As demonstrated, the DR-HBNM is a boundary-only meshless approach. No boundary elements are used for both interpolation and integration purpose. The nodes in the domain are needed just for interpolation for the particular solutions, which cannot influence the present method as a boundary-type method.

4. Numerical examples

A few illustrative numerical results from DR-HBNM, together with comparisons with exact solutions, follow. In all cases, the Helmholtz equation

$$\nabla^2 u = -\mu^2 u$$

is solved, together with appropriate prescribed boundary conditions. For the purpose of error estimation and convergence studies, the relative error is defined as

$$e = \frac{|u^{(n)} - u^{(e)}|}{u^{(e)}} \tag{59}$$

where the superscripts (e) and (n) refer to the exact and the numerical solutions, respectively.

In all examples, the support size for the weight function $\hat{d}_I$ is set to be $3.5q$, with q being the average distance of adjacent nodes. The parameter c_I is taken to be $d_I/c_I = 0.5$. In this paper, $r_I = 0.85q$ is chosen as the radius of the sub-domain, and the parameter c_J is taken to be $r_J/c_J = 1.1$. In order to deal with the normal flux discontinuities at the corners, the nodes are not arranged at these places and the support domain for interpolation is truncated. In order to present the performance of the numerical method proposed, we consider the following vibrating beams with two different boundary conditions. In this case, u represents displacement and $\mu^2 = \rho\omega^2/E$ where ρ and E are material properties and ω are the natural frequencies.

4.1. Clamped–free beam

Consider the vibrating beam shown in Fig. 2. The beam is 0.9 m long and is discretized using 40 boundary nodes and 24 internal nodes. A small arbitrary displacement u_0 was imposed at the boundary node at the middle of the clamped side (node 40), while at all the remaining nodes the condition $t = 0$ was prescribed. The exact solution for the natural frequencies is given by

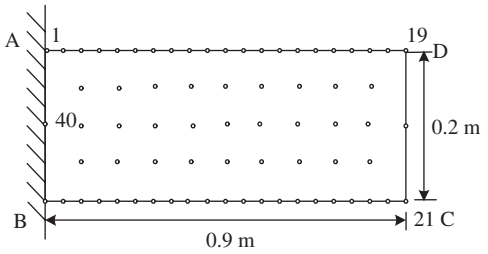

Fig. 2. DR-HBNM discretization of the clamped–free beam.

$$\mu_m = \frac{\pi}{l}\left(m - \frac{1}{2}\right) \tag{60}$$

Considering the problem as one dimensional, the deformed shape is then given by

$$u_m = C\sin\left[\left(m - \frac{1}{2}\right)\frac{\pi x}{l}\right] \tag{61}$$

where m is an integer which takes values up to the desired order, l is the length of the beam and C is an arbitrary constant. From Eq. (60) the natural frequencies of the beam can be calculated by the expression

$$\omega^2 = \frac{E\mu^2}{\rho} \tag{62}$$

where ρ and E are material constants. Eq. (61) gives the deformed shape for a given μ_m once C is defined. In all the examples, $C = 1$.

Eq. (48) was solved starting from $\mu = 0$ using a variable step on μ. The program starts with $\Delta\mu = 0.1$, if for two successive iterations the average increase in the value of u at all the nodes is more than 30%, then $\Delta\mu$ is decreased to 0.01. When mean values of u started to drop, $\Delta\mu$ was increased to 0.5. This value was used until values of u started to increase again.

In the present calculation, the boundary of the vibrating beam is divided into four piecewise smooth segments. The regular meshes of 40 nodes (19 nodes on AD and BC each, 1 node on AB and CD each) on the boundary ($N = 40$) and 24 internal nodes ($L = 24$) are used, which are shown in Fig. 2. The deformed shapes of the beam for the first four natural frequencies are plotted in Fig. 3. In order to test the efficacy of the method, the results of the DR-HBNM and the analytical solution are shown for comparison. It can be observed from these figures that the present method gives very good results for the problem.

In order to test the sensitivity of the DR-HBNM to the number of boundary nodes and the number of the internal nodes, seven other discretizations were applied. The relative errors for each nodal arrangement in the DR-HBNM computations are presented in Fig. 4. It can be seen that for this type of problem the use of a number of internal nodes is advisable, especially for higher vibration modes.

4.2. Clamped–clamped beam

Consider the vibrating beam shown in Fig. 5. The beam is 0.9 m long and the nodal arrangement is the same as the example above. A small arbitrary displacement u_0 was also imposed at the boundary node at the middle of the clamped side (node 40) on the left boundary, while at all the remaining nodes the condition $t = 0$ was prescribed. The exact solution for the natural frequencies is given by

$$\mu_m = \frac{m\pi}{l} \tag{63}$$

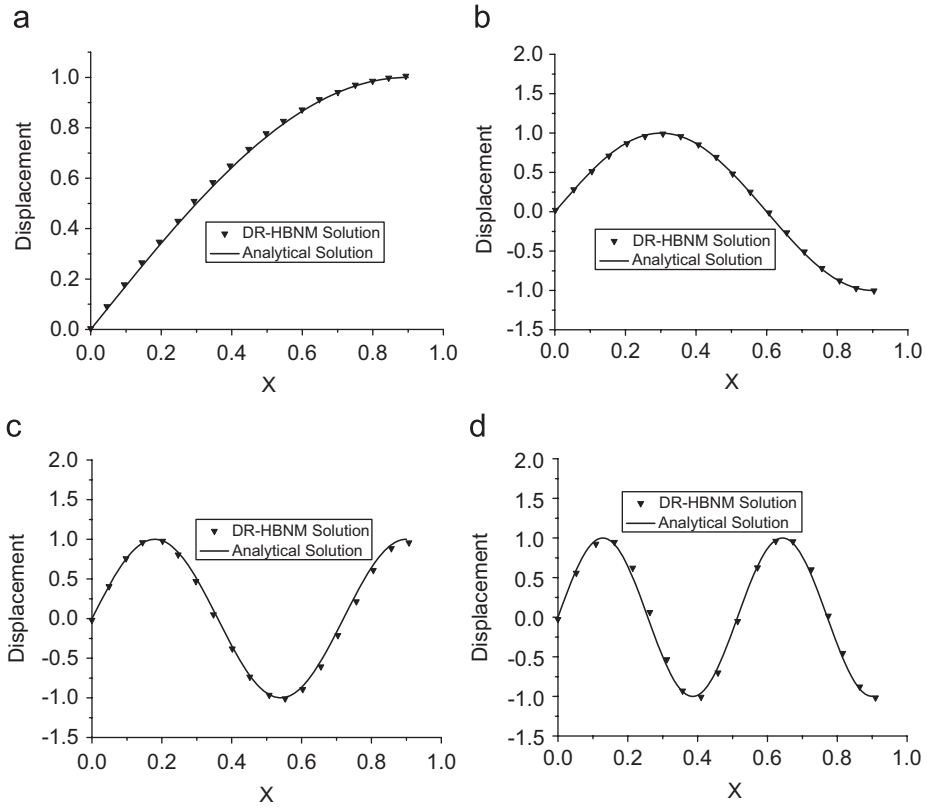

Fig. 3. Deformed shape for first four natural frequencies of clamped–free beam.

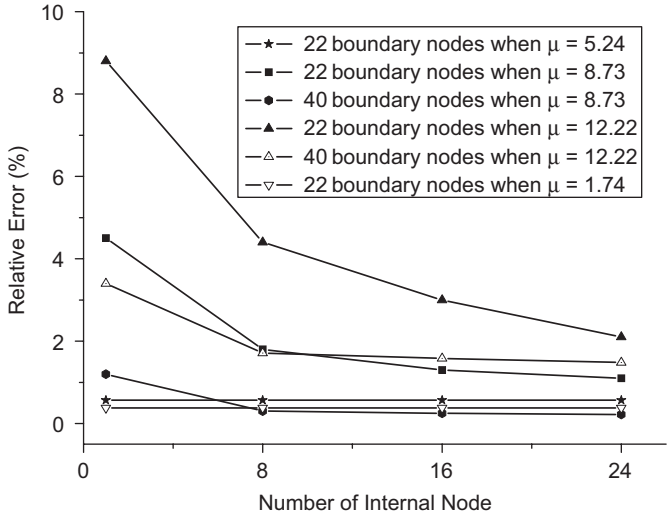

Fig. 4. Relative error for μ for clamped–free beam with different discretization.

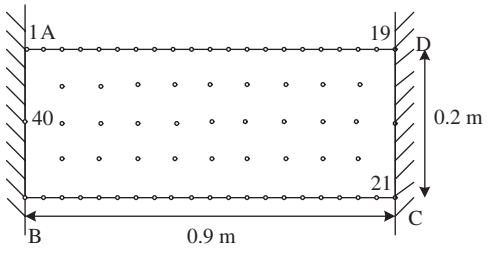

Fig. 5. DR-HBNM discretization of the clamped–clamped beam.

Considering the problem as one dimensional, the deformed shape is then given by

$$u_m = C\sin\left(\frac{m\pi x}{l}\right) \tag{64}$$

In the present calculation, the discretization of the domain is the same as the first examples, which are shown in Fig. 5. The deformed shapes of the beam for the first four natural frequencies are plotted in Fig. 6. In order to test the efficacy of the method, the results of the DR-HBNM and the analytical solution are shown for comparison. To study the convergence of the method, different number of boundary nodes and internal nodes are used. The numerical results of μ from the DR-HBNM together with the exact solution are shown in Table 1. It can be seen that the present method has high rates of convergence and the agreement between numerical and exact results are excellent.

5. Conclusions

A truly meshless method for solving the Helmholtz-type equation, which is called DR-HBNM, has been presented in this paper. This method combines the DRM and hybrid BNM. The hybrid BNM is used to solve the homogeneous equations, and the DRM is employed to solve the inhomogeneous terms. No cells are needed either for the interpolation purposes or for integration process, only discrete nodes are constructed on the boundary of a domain, several nodes in the domain are needed just for the RBF interpolation.

The internal nodes used in the present method are usually defined at positions where the solution is required. The use of a number of internal nodes is important in most cases especially for higher vibration modes. Results are normally not very sensitive to

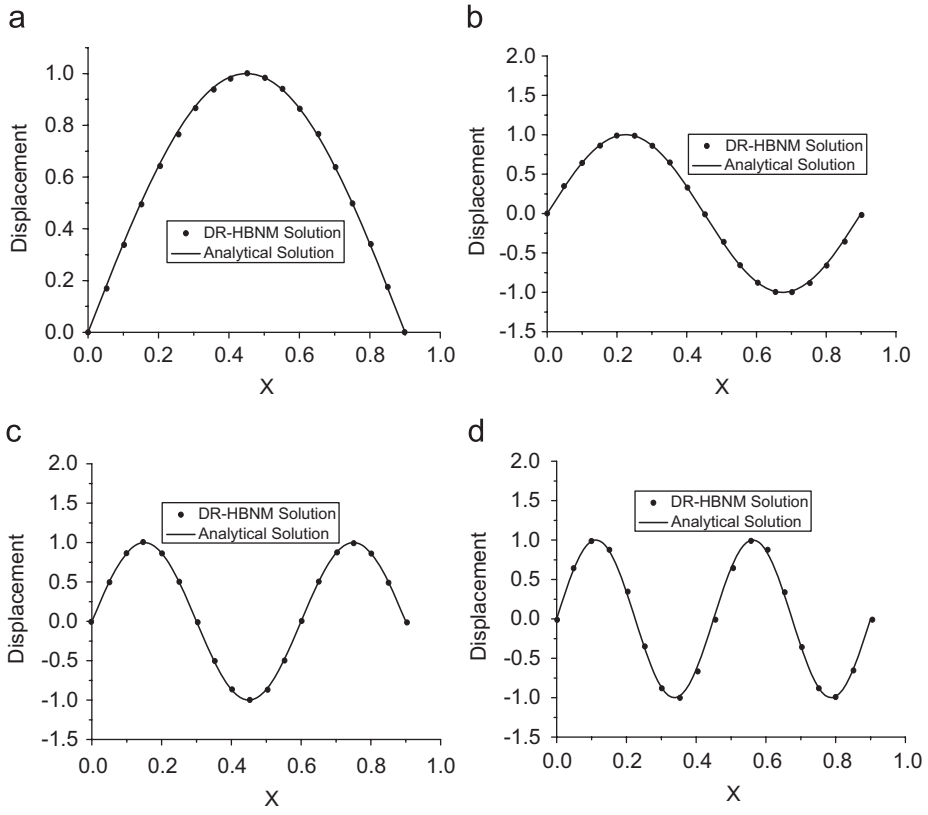

Fig. 6. Deformed shape for first four natural frequencies of clamped–clamped beam.

Table 1
Results for μ for clamped–clamped beam using different discretization

μ, Exact	$N = 22$				$N = 40$			
	20 Nodes on AD and BC and 2 nodes on AB and CD				38 Nodes on AD and BC and 2 nodes on AB and CD			
	$L = 1$	$L = 8$	$L = 16$	$L = 24$	$L = 1$	$L = 8$	$L = 16$	$L = 24$
3.49	3.49	3.50	3.50	3.50	3.48	3.49	3.49	3.49
6.98	7.11	7.04	7.04	6.99	6.99	6.99	6.99	6.98
10.47	11.08	10.70	10.65	10.61	10.80	10.54	10.51	10.49
13.96	15.09	14.76	14.60	14.44	15.03	14.27	14.11	14.03

number and location of the internal nodes and in lower vibration modes which can be determined by a convergence test. Based on the numerical examples, the number of internal nodes $L = N/2$, where N is the number of boundary nodes, provides solutions which are satisfactory for all problems.

The DR-HBNM has been verified and the size of the sub-domain radius is studied through the numerical examples. It is observed that the optimal value of the radius of the sub-domain is between 0.8 and 0.9h.

The numerical examples of a vibrating beam with different boundary conditions have been given and the numerical results have demonstrated the accuracy and convergence of the present method. The serious 'boundary-layer effect' in the hybrid BNM is circumvented by the adaptive integration scheme. Furthermore, it can be extended to the other complicated inhomogeneous equations.

References

[1] Beskos DE. Boundary element method in dynamic analysis: part II (1986–1996). ASME Appl Mech Rev 1997;50:149–97.
[2] Chen JT, Wong FC. Dual formulation of multiple reciprocity method for the acoustic mode of a cavity with a thin partition. J Sound Vib 1998; 217:75–95.
[3] Harari I, Barbone PE, Slavutin M, Shalom R. Boundary infinite elements for the Helmholtz equation in exterior domains. Int J Numer Meth Eng 1998;41: 1105–31.
[4] Hall WS, Mao XQ. A boundary element investigation of irregular frequencies in electromagnetic scattering. Eng Anal Boundary Elem 1995;16:245–52.
[5] Partridge PW, Brebbia CA, Wrobel LW. The dual reciprocity boundary element method. Southampton: Computational Mechanics Publication; 1992.
[6] Nowak AJ, Neves AC, editors. The multiple reciprocity boundary element method. Southampton: Computational Mechanics Publication; 1994.
[7] Nowak AJ, Partridge PW. Comparison of the dual reciprocity and the multiple reciprocity methods. Eng Anal Boundary Elem 1992;10:155–60.
[8] Mukherjee YX, Mukherjee S. The boundary node method for potential problems. Int J Numer Meth Eng 1997;40:797–815.
[9] Zhang JM, Yao ZH, Li H. A hybrid boundary node method. Int J Numer Meth Eng 2002;53:751–63.
[10] Zhang JM, Yao ZH, Masataka Tanaka. The meshless regular hybrid boundary node method for 2-D linear elasticity. Eng Anal Bound 2003;127: 259–68.
[11] Zhang JM, Yao ZH. The regular hybrid boundary node method for three-dimensional linear elasticity. Eng Anal Boundary Elem 2004;28:525–34.
[12] Zhang JM, Masataka Tanaka, Toshiro Matsumoto. Meshless analysis of potential problems in three dimensions with the hybrid boundary node method. Int J Numer Meth Eng 2004;59:1147–68.

[13] Lancaster P, Salkauskas K. Surfaces generated by moving least squares methods. Math Comput 1981;37:41–58.
[14] Nardini D, Brebbia CA. Transient dynamic analysis by the boundary element method. In: Boundary element methods in engineering. Southampton, Berlin and New York: Computational Mechanics Publications, Springer; 1983.
[15] Wrobel LC, Brebbia CA. The dual reciprocity boundary element formulation for non-linear diffusion problems. Comput Meth Appl Mech Eng 1987;65(2):147–64.
[16] Mukherjee YX, Mukherjee S. On boundary conditions in the element-free Galerkin method. Comput Mech 1997;19:264–70.
[17] Miao Y, Wang YH, Yu F. Development of hybrid boundary node method in two-dimensional elasticity. Eng Anal Boundary Elem 2005;29:703–12.